
Regularized Langevin Dynamics for Combinatorial Optimization

Shengyu Feng¹ Yiming Yang¹

Abstract

This work proposes a simple yet effective sampling framework for combinatorial optimization (CO). Our method builds on discrete Langevin dynamics (LD), an efficient gradient-guided generative algorithm. However, we observed that directly applying LD often leads to limited exploration. To overcome this limitation, we propose the *Regularized Langevin Dynamics (RLD)*, which enforces an expected distance between the sampled and current solutions, effectively avoiding local minima. We develop two CO solvers on top of RLD, one based on simulated annealing (SA) and the other one based on neural network (NN). Empirical results on three classical CO problems demonstrate that both of our methods can achieve comparable or better performance against the previous state-of-the-art (SOTA) SA and NN-based solvers. In particular, our SA algorithm reduces the running time of the previous SOTA SA method by up to 80%, while achieving equal or superior performance. In summary, RLD offers a promising framework for enhancing both traditional heuristics and NN models to solve CO problems.

1. Introduction

Combinatorial Optimization (CO) problems are central challenges in computer science and operations research (Papadimitriou & Steiglitz, 1998), with diverse real-world applications such as supply chain management, logistics optimization (Chopra & Meindl, 2001), workforce scheduling (Ernst et al., 2004), financial portfolio management (Rubinstein, 2002; Lobo et al., 2007), compiler optimization (Trofin et al., 2021; Zheng et al., 2022), and bioinformatics (Gusfield, 1997). Despite their wide-ranging utility, CO problems are inherently difficult due to their non-convex nature and often NP-hard complexity, making them intractable in polynomial time by exact solvers. Traditional CO algo-

rithms often rely on hand-crafted, domain-specific heuristics, which are costly and difficult to design, posing significant challenges in solving novel or complex CO problems.

Recent advancements in neural network (NN)-based learning (Bengio et al., 2020) and simulated annealing (SA) (Kirkpatrick et al., 1983) algorithms have redefined approaches to combinatorial optimization by minimizing dependence on manual heuristics:

- **Neural Network Models:** NN-based methods leverage reinforcement learning (Khalil et al., 2017; Qiu et al., 2022), unsupervised learning (Karalias & Loukas, 2020a; Wang et al., 2022; Wang & Li, 2023; Sanokowski et al., 2024) or generative models (Kool et al., 2019; Zhang et al., 2023; Sun & Yang, 2023; Li et al., 2023; 2024) to learn optimization strategies directly from data. By automating the process, these models replace handcrafted heuristics with learned representations and decision-making processes, enabling tailored solutions refined through training rather than manual adjustment.
- **Simulated Annealing:** SA is a general-purpose optimization algorithm that explores the solution space probabilistically, avoiding dependence on problem-specific heuristics. Although its cooling schedule and acceptance criteria require some design decisions, SA is highly adaptable across diverse problems free from detailed domain knowledge (Johnson et al., 1991).

Discrete Langevin dynamics (LD) (Zhang et al., 2022; Sun et al., 2022) and the corresponding diffusion models (Chen et al., 2023; Austin et al., 2021) have greatly advanced the recent development of both NN and SA solvers. The key idea of LD is to guide the iterative sampling via the gradient, for a more efficient searching/generation process. For instance, DIFUSCO (Sun & Yang, 2023) adopts continuous diffusion models from computer vision to address the discrete nature of CO problems, outperforming previous end-to-end neural models in both accuracy and computational efficiency. Additionally, DiffUCO (Sanokowski et al., 2024) generalizes DIFUSCO by eliminating the need for labeled training data, using unsupervised learning for CO problems. Meanwhile, advanced SA-based CO solvers have demonstrated performance on par with state-of-the-art NN-based approaches.

¹Language Technologies Institute, Carnegie Mellon University. Correspondence to: Shengyu Feng <shengyuf@cs.cmu.edu>.

Sun et al. (2023) underscore the advantages of LD-based SA method, including their simplicity, superior speed-quality trade-offs, and generalizability to new CO problems, as they require no training or problem-specific customization. However, existing discrete LD/diffusion methods are all adapted from the methods (Welling & Teh, 2011; Sohl-Dickstein et al., 2015; Song & Ermon, 2019; Ho et al., 2020; Song & Ermon, 2020) in the continuous domain, this raises important questions: Is there any difference between CO and continuous optimization? Do these adapted methods sufficiently consider the nature of discrete data? Exploring these questions is the central focus of this paper.

Our key observation is that the optimization process is more prone to local optima in a discrete domain than in a continuous one. That is, local optima in a continuous domain typically has a zero gradient (under the smoothness condition) but this is often not true in a discrete domain, where the gradients may be very large in magnitude but pointing to an infeasible region. Such a difference makes the escaping of local optima more difficult in a discrete domain than in a continuous one, with the common strategy of adding a random noise as in LD. We propose to address this issue by enforcing a constant norm of the expected distance between the sampled solution and the current solution during the searching process. In other words, we control the magnitude of the update in LD, encouraging the search to explore more promising areas. We name this sampling method *Regularized Langevin Dynamics (RLD)*. We apply RLD on both SA and NN-based CO solvers, leading to Regularized Langevin Simulated Annealing (RLSA) and Regularized Langevin Neural Network (RLNN). Our empirical evaluation on three CO problems demonstrate this significant improvement of RLSA and RLNN over both SA and NN baselines. Notably, RLSA only needs 20% running time to outperform the previous SOTA SA baselines. It shows a clear efficiency advantage with either less or more searching steps.

To summarize, we propose a new variant of discrete Langevin dynamics for CO by regularizing the expected update magnitude on the current solution at each step. Our method is featured by its simplicity, effectiveness, and wide applicability to both SA and NN-based solvers, indicating its strong potential in addressing CO problems.

2. Preliminary

2.1. Combinatorial Optimization Problems

Following Papadimitriou & Steiglitz (1982), we formulate the combinatorial optimization (CO) problem as a constrained optimization problem, i.e.,

$$\min_{\mathbf{x} \in \{0,1\}^N} a(\mathbf{x}) \quad \text{s.t.} \quad b(\mathbf{x}) = 0, \quad (1)$$

where $a(\mathbf{x})$ stands for the target to optimize and $b(\mathbf{x}) \geq 0$ corresponds to the amount of constraint violation (0 means no violation). In particular, we focus on the penalty form that can be written as

$$\min_{\mathbf{x} \in \{0,1\}^N} H(\mathbf{x}) = a(\mathbf{x}) + \beta b(\mathbf{x}), \quad (2)$$

where $\beta > 0$ is the penalty coefficient that should be sufficiently large, such that the minima of Equation 2 corresponds to the feasible solutions in Equation 1. $H(\mathbf{x})$ is also generally named as the energy function, and its associated energy-based model (EBM) is defined as

$$p_\tau(\mathbf{x}) = \frac{\exp(-H(\mathbf{x})/\tau)}{Z}, \quad (3)$$

where $\tau > 0$ is the temperature controlling the smoothness of the distribution, and $Z = \sum_{\mathbf{x} \in \{0,1\}^N} \exp(-H(\mathbf{x})/\tau)$ is the normalization factor, typically intractable. When τ is small, the probability mass of p_τ tends to concentrate around low-energy samples, making the task of solving Equation 1 equivalent to sampling from $p_\tau(\mathbf{x})$. Markov Chain Monte Carlo (MCMC) (Lecun et al., 2006) is the most widely used method for sampling from the EBM defined above. However, directly applying MCMC may lead to inefficiencies due to the non-smoothness introduced by the small τ . To mitigate this issue, the simulated annealing (SA) technique is commonly employed to gradually decrease τ towards zero during the MCMC process.

2.2. Langevin Dynamics

Langevin dynamics (LD) (Welling & Teh, 2011) is an efficient MCMC algorithm initially developed in the continuous domain. It takes a noisy gradient ascent update at each step to gradually increase the log-likelihood of the sample:

$$\mathbf{x}' = \mathbf{x} + \frac{\alpha}{2} s(\mathbf{x}) + \sqrt{\alpha} \zeta, \quad \zeta \in \mathcal{N}(0, \mathbf{I}_{N \times N}), \quad (4)$$

where $s(\mathbf{x}) = \nabla \log p(\mathbf{x})$ is known as the score function (gradient of the log likelihood), and $\alpha > 0$ represents the step size. By iteratively performing the above update, the sample \mathbf{x} would eventually end up at a stationary distribution approximately equal to $p(\mathbf{x})$.

Recently, Zhang et al. (2022) have extended LD to discrete space by rewriting Equation 4 as

$$q(\mathbf{x}'|\mathbf{x}) = \frac{\exp(-\frac{1}{2\alpha} \|\mathbf{x}' - \mathbf{x} - \frac{\alpha}{2} s(\mathbf{x})\|_2^2)}{Z(\mathbf{x})}, \quad (5)$$

where $Z(\mathbf{x})$ is the normalization factor. For discrete data, the above distribution could be factorized coordinatewisely, i.e., $q(\mathbf{x}'|\mathbf{x}) = \prod_{i=1}^N q(\mathbf{x}'_i|\mathbf{x}_i)$, into a set of categorical distributions:

$$q(\mathbf{x}'_i|\mathbf{x}_i) \propto \exp\left(\frac{1}{2} s(\mathbf{x})_i (\mathbf{x}'_i - \mathbf{x}_i) - \frac{(\mathbf{x}'_i - \mathbf{x}_i)^2}{2\alpha}\right). \quad (6)$$

When \mathbf{x} is a binary vector, we can obtain the flipping (changing the value of \mathbf{x}_i from 0 to 1, or 1 to 0) probability $q(\mathbf{x}'_i = 1 - \mathbf{x}_i | \mathbf{x})$ as

$$\text{Sigmoid}\left(\frac{1}{2}s(\mathbf{x})_i(1 - 2\mathbf{x}_i) - \frac{1}{2\alpha}\right). \quad (7)$$

In particular, it can be shown that the discrete Langevin sampler is a first-order approximation to the locally-informed proposal (Zanella, 2017) in the following form.

$$q(\mathbf{x}'_i | \mathbf{x}) \propto \exp\left(\frac{1}{2}p(\mathbf{x}') - \frac{1}{2}p(\mathbf{x}) - \frac{(\mathbf{x}'_i - \mathbf{x}_i)^2}{2\alpha}\right). \quad (8)$$

3. Method

3.1. Regularized Langevin Dynamics

How to select the step size α is critical to the effectiveness of LD for CO. In this work, we propose to select α by regularizing the update with the L2 distance¹ between the sampled and current solutions:

$$q(\mathbf{x}'_i | \mathbf{x}) \propto \exp\left(\frac{1}{2}s(\mathbf{x})_i(\mathbf{x}'_i - \mathbf{x}_i) - \frac{(\mathbf{x}'_i - \mathbf{x}_i)^2}{2\alpha}\right), \quad (9)$$

s.t. $\mathbb{E}_{q(\mathbf{x}' | \mathbf{x})}[\|\mathbf{x}' - \mathbf{x}\|_2] = d,$

where d is a positive integer. When \mathbf{x} is binary, we could explicitly write out the expectation in Equation 9 with the flipping probability $q(\mathbf{x}'_i = 1 - \mathbf{x}_i | \mathbf{x})$:

$$\sum_{i=1}^N \text{Sigmoid}\left(\frac{1}{2}s(\mathbf{x})_i(1 - 2\mathbf{x}_i) - \frac{1}{2\alpha}\right) = d. \quad (10)$$

We find this simple regularization method very effective in mitigating the local optima issue in CO, in the sense that the regularization term enforces the change of a fixed magnitude to the solution, regardless of the gradient. We name our method as *Regularized Langevin Dynamics (RLD)*, and we proceed to introduce its applications in both SA and NN-based CO solvers.

3.2. Regularized Langevin Simulated Annealing

Since the gradient of the energy function could be computed in an closed form for various CO problems, here we first assume $\nabla H(\mathbf{x})$ is available. Note that the score function of the EBM could be written as $s_\tau(\mathbf{x}) = \log p_\tau(\mathbf{x}) = -\frac{1}{\tau}\nabla H(\mathbf{x})$. To avoid the clutter, we denote $\Delta = (2\mathbf{x} - 1) \odot \nabla H(\mathbf{x})$, whose i -th coordinate approximates the drop of the energy function if we flip the value of \mathbf{x}_i .

Explicitly solving Equation 10 is challenging due to the presence of the sigmoid function. However, when $\tau \rightarrow 0$,

¹there is no difference between L1 and L2 distances on binary data, we leave the choice on other discrete data as future study.

the sigmoid function is approximately an indicator function:

$$\lim_{\tau \rightarrow 0} \text{Sigmoid}\left(\frac{1}{2\tau}\Delta_i - \frac{1}{2\alpha}\right) = \mathbb{1}\left(\frac{1}{2\tau}\Delta_i - \frac{1}{2\alpha} > 0\right). \quad (11)$$

This property allows us to efficiently regularize the SA algorithm with the d -th largest element in Δ , denoted as $\Delta_{(d)}$.

We then obtain the flipping probability by letting $\frac{1}{\alpha} = \frac{\Delta_{(d)}}{\tau}$:

$$q(\mathbf{x}'_i = 1 - \mathbf{x}_i | \mathbf{x}) = \text{Sigmoid}\left(\frac{1}{2\tau}(\Delta_i - \Delta_{(d)})\right). \quad (12)$$

In our experiment, we find simply ignoring $-\frac{1}{\alpha}$ and normalizing all sigmoid function outputs to sum to d could also work, followed by clipping all values into the range $[0, 1]$. While in this work we just stick to using the d -th largest element. We call the resultant SA algorithm as *Regularized Langevin Simulated Annealing (RLSA)*, whose details are summarized in Algorithm 1.

Algorithm 1 Regularized Langevin Simulated Annealing

```

1: Input:  $T, d$  and  $\tau_0$ 
2: Initialize  $\mathbf{x} \in \{0, 1\}^N$ ;  $\mathbf{x}^* \leftarrow \mathbf{x}$ 
3: for  $t = 1, \dots, T$  do
4:    $\tau \leftarrow \tau_0(1 - \frac{t-1}{T})$ 
5:    $\Delta \leftarrow (2\mathbf{x} - 1) \odot \nabla H(\mathbf{x})$ 
6:   for  $i = 1, \dots, N$  do
7:      $p \leftarrow \text{Sigmoid}(\frac{1}{2\tau}(\Delta_i - \Delta_{(d)}))$ 
8:      $c \sim \text{Bernoulli}(p)$ 
9:      $\mathbf{x}_i \leftarrow \mathbf{x}_i(1 - c) + (1 - \mathbf{x}_i)c$ 
10:  end for
11:  if  $H(\mathbf{x}) < H(\mathbf{x}^*)$  then
12:     $\mathbf{x}^* \leftarrow \mathbf{x}$ 
13:  end if
14: end for
15: return  $\mathbf{x}^*$ 

```

In our implementation, the elementwise sampling is run in parallel and we maintain K independent SA processes simultaneously. The whole algorithm could be implemented in a few lines and accelerated with GPU-based deep learning frameworks, such as PyTorch (Paszke et al., 2017) and Jax (Bradbury et al., 2018). In this work, we implement our algorithm mainly based on PyTorch Geometric (Fey & Lenssen, 2019), and an example code is attached in Appendix C.

Given the overall RLSA framework, we now address the question of how to compute the gradient of the energy function. Numerous classical CO problems are defined over graphs and could be formulated in quadratic form, known as QUBO (Lucas, 2014). Let $\mathcal{G} = (\mathcal{V}, \mathcal{E})$ be an undirected graph, with node set $\mathcal{V} = \{1, \dots, N\}$, edge set $\mathcal{E} \in \mathcal{V} \times \mathcal{V}$, and adjacency matrix $\mathbf{A} \in \{0, 1\}^{N \times N}$. In this work, we focus on the following three problems, which have been commonly used in benchmark evaluations for CO solvers.

Maximum Independent Set. The maximum independent set (MIS) problem aims to select the largest subset of nodes from the graph \mathcal{G} , without any adjacent pair. Denote a selected node as $\mathbf{x}_i = 1$ and an unselected one as $\mathbf{x}_i = 0$, the energy function of MIS could be expressed as

$$\begin{aligned} H(\mathbf{x}) &= -\sum_{i=1}^N \mathbf{c}_i \mathbf{x}_i + \beta \sum_{(i,j) \in \mathcal{E}} \mathbf{x}_i \mathbf{x}_j \\ &= -\mathbf{c}^\top \mathbf{x} + \beta \frac{\mathbf{x}^\top \mathbf{A} \mathbf{x}}{2}, \end{aligned} \quad (13)$$

where $\mathbf{c} \in \mathbb{R}_+^N$ is the node weight vector. It is not hard to compute the gradient of the energy function as

$$\nabla H(\mathbf{x}) = -\mathbf{c} + \beta \mathbf{A} \mathbf{x}. \quad (14)$$

Maximum Clique. The maximum clique (MCI) stands for the largest subset of nodes in a graph such that every two nodes in the set are adjacent to each other. It could actually be expressed as the MIS problem in the complete graph, with the energy function:

$$H(\mathbf{x}) = -\sum_{i=1}^N \mathbf{c}_i \mathbf{x}_i + \beta \sum_{(i,j) \notin \mathcal{E}} \mathbf{x}_i \mathbf{x}_j. \quad (15)$$

In order to represent the energy function with the adjacency matrix \mathbf{A} , we rewrite the penalty as $[\sum_{i=1}^N \mathbf{x}_i]^2 - \sum_{i=1}^N \mathbf{x}_i^2]/2 - \sum_{(i,j) \in \mathcal{E}} \mathbf{x}_i \mathbf{x}_j$, resulting in the energy function and its gradient:

$$H(\mathbf{x}) = \mathbf{c}^\top \mathbf{x} + \beta \frac{(\mathbf{1}^\top \mathbf{x})^2 - \mathbf{x}^\top \mathbf{x} - \mathbf{x}^\top \mathbf{A} \mathbf{x}}{2}, \quad (16)$$

$$\nabla H(\mathbf{x}) = -\mathbf{c} + \beta((\mathbf{1}^\top \mathbf{x})\mathbf{1} - \mathbf{x} - \mathbf{A} \mathbf{x}). \quad (17)$$

Max Cut. The max cut (MCut) problem looks to partition the nodes into two sets so that the number of edges between two sets is maximized. Here we use $\mathbf{x}_i = 1$ and $\mathbf{x}_i = 0$ to represent the belonging to two sets, and the energy function could be expressed as

$$\begin{aligned} H(\mathbf{x}) &= -\sum_{(i,j) \in \mathcal{E}} \frac{1 - (2\mathbf{x}_i - 1)(2\mathbf{x}_j - 1)}{2} \\ &= \mathbf{x}^\top \mathbf{A} \mathbf{x} - \mathbf{1}^\top \mathbf{A} \mathbf{x}, \end{aligned} \quad (18)$$

whose gradient could be accordingly computed as

$$\nabla H(\mathbf{x}) = \mathbf{A}(2\mathbf{x} - \mathbf{1}). \quad (19)$$

3.3. Regularized Langevin Neural Network

When the gradient is intractable or a better approximation of the locally-informed proposal in Equation 8 is wanted, we could parameterize the sampling distribution $q_\theta(\mathbf{x}'|\mathbf{x})$ with a

NN. Here we still utilize a mean-field decomposition, letting $q_\theta(\mathbf{x}'|\mathbf{x}) = \prod_{i=1}^N q_\theta(\mathbf{x}'_i|\mathbf{x})$. The RLD update in Equation 9 could be translated into the following training loss

$$\begin{aligned} l_{RLD}(\theta; \mathbf{x}, d, \lambda) &= \mathbf{E}_{q_\theta(\mathbf{x}'|\mathbf{x})}[H(\mathbf{x}')] \\ &\quad + \lambda \left(\sum_i^N q_\theta(\mathbf{x}'_i = 1 - \mathbf{x}_i|\mathbf{x}) - d \right)^2. \end{aligned} \quad (20)$$

Here the first term is similar to the loss function used in the Erdoes Goes Neural (Karalias & Loukas, 2020b), which maximizes the conditional expectation of the energy function after the update. While the second term regularizes the expected Hamming distance between the two solutions, with λ being the regularization coefficient. We name this NN-based solver as *Regularized Langevin Neural Network (RLNN)*.

We train RLNN in a similar fashion to reinforcement learning through sampling and update, but without the need to account the future states except the immediate next one. This allows RLNN to circumvent the high variance in estimating the future return when trained with a long sampling process. In detail, each time we sequentially samples T' samples with the current proposal distribution $q_\theta(\mathbf{x}'|\mathbf{x})$, then for each sample, we train RLNN to minimize the loss in Equation 20. The training algorithm is summarized in Algorithm 2.

Algorithm 2 Regularized Langevin Neural Network (train)

```

1: Input:  $T', d, \lambda$ 
2: Initialize  $\theta$ 
3: while the stopping criterion is not met do
4:   Initialize  $\mathbf{x} \in \{0, 1\}^N, \mathcal{D} = \{\mathbf{x}\}$ 
5:   for  $t = 1, \dots, T'$  do
6:      $\mathbf{x}' \sim q_\theta(\mathbf{x}'|\mathbf{x})$ 
7:      $\mathcal{D} \leftarrow \mathcal{D} \cup \{\mathbf{x}'\}$ 
8:      $\mathbf{x} \leftarrow \mathbf{x}'$ 
9:   end for
10:   $\theta \leftarrow \min_\theta \mathbf{E}_{\mathbf{x} \in \mathcal{D}}[l_{RLD}(\theta; \mathbf{x}, d, \lambda)]$ 
11: end while
12: return  $\theta$ 

```

Similarly, we maintain K' parallel sampling processes in our implementation to obtain more efficient training data collection. During the inference time, we simply sample from $q_\theta(\mathbf{x}'|\mathbf{x})$ sequentially for T steps with K' processes run in parallel. Note that temperature annealing is not used here as we do not find it useful and we simply leave $\tau = 1$.

3.4. Connection to Normalized Gradient Descent

Our proposed RLD method is closely related to the normalized gradient descent (NGD) method (Cortés, 2006) in the

continuous domain:

$$\mathbf{x}' = \mathbf{x} - \alpha \frac{\nabla f(\mathbf{x})}{\|\nabla f(\mathbf{x})\|_2}. \quad (21)$$

NGD is developed to address the vanishing/exploding gradient by normalizing the L2 norm of the gradient for a scale-invariant update at each step. Our method could be treated as a discrete version of method by restricting the L2 distance between the solutions before and after the update.

The key difference between the two lies in the case when $\Delta_{(d)} < 0$, RLD could not be translated into a gradient descent algorithm in Equation 4 (in terms of minimizing the energy function) since $\alpha = \frac{\tau}{\Delta_{(d)}} < 0$ reverses the gradient descent direction. Instead, this should be treated as a way to escape the local optima without dramatically increasing the energy function. As an analogy to Equation 5, we can express this situation as

$$q(\mathbf{x}'|\mathbf{x}) = \frac{\exp(-\frac{\Delta_{(d)}}{2\tau}\|\mathbf{x}' - \mathbf{x} + \frac{1}{2\Delta_{(d)}}H(\mathbf{x})\|_2^2)}{Z(\mathbf{x})}. \quad (22)$$

The density of $q(\mathbf{x}'|\mathbf{x})$ increases with respect to the distance from $\mathbf{x} - \frac{1}{2\Delta_{(d)}}H(\mathbf{x})$, which is the **gradient ascent direction** (note $\Delta_{(d)}$ is negative here) of the energy function. This behavior arises due to the different property of the local optima in the discrete data, which may not vanish to 0 but point to an infeasible region (with Δ negative in all dimensions).

Let us take MIS as an example, whose local optima is a maximal independent set, i.e., each unselected node has at least one neighbor in the set. The gradient for the selected node ($\mathbf{x}_i = 1$) is $\nabla H(\mathbf{x})_i = -\mathbf{c}_i < 0$, pointing to the direction of increasing the value, which is infeasible as $\mathbf{x}_i \leq 1$. While the gradient for an unselected node ($\mathbf{x}_i = 0$) is lower bounded by $\nabla H(\mathbf{x})_i \geq -\mathbf{c}_i + \beta > 0$, pointing to the direction of decreasing the value, which is also infeasible. Since the gradient descent direction is not informative, RLD would try to escape this local optima but avoid the steepest direction to increase the energy function, which is exactly the gradient ascent direction: $\mathbf{x} - \frac{1}{2\Delta_{(d)}}H(\mathbf{x})$.

With the same example, we could also see why the standard discrete Langevin sampler (Zhang et al., 2022) with a constant step size does work well. Since LD is a first-order approximation of the locally-informed proposal (Zanella, 2017), a small α is needed to make the approximation accurate. However, a small α would also lead to a strong penalization on the update. While at the local optima, we also have $\Delta_i < 0$ discourage the change, as indicated in Equation 7. Therefore, additional efforts are needed to help LD escape the local optima beyond the force of random noise. Such a distinction between CO and continuous optimization highlights the significance of RLD.

4. Experiments

4.1. Experimental Setup

Benchmark datasets. Following Zhang et al. (2023), we use the Revised Model B (RB) graphs (Xu & Li, 2000) for the evaluation of MIS and MCI problems, and use the Barabasi-Albert (BA) graphs (Barabási & Albert, 1999) for the evaluation of MCI problem. In addition, we also include Erdős-Rényi (ER) graphs (Erdos & Rényi, 1984) used by Qiu et al. (2022) on the MIS problem. We follow the above works to generate RB, BA and ER graphs at two different scales. On RB and BA graphs, the small scale contains 200 to 300 nodes and the large scale contains 800 to 1200 nodes. While the ER graphs have a small scale of 700 to 800 nodes and a large scale of 9,000 to 11,000 nodes. The large-scale ER graphs are used for transfer testing on the models trained on the small-scale ER graph. A suffix of ‘-[$n-N$]’ is used to differentiate the graphs with different scales, implying that the graphs contain n to N nodes. The test set size is 500 for RB and BA graphs, 128 for ER-[700–800] and 16 for ER-[9000–11000]. A training set of size 1000 and validation set of 500 graphs is used for all datasets except for ER-[9000–11000]. The node weight in MIS and MCI is set as 1 for all nodes.

Baselines. Following Qiu et al. (2022) and Zhang et al. (2023), we categorize our baselines as the classical operation research methods (OR), heuristic methods (H), reinforcement learning-based solvers (RL), supervised learning-based solvers (SL) and unsupervised learning-based solvers (UL). For MIS, we have the integer linear programming solver Gurobi (Gurobi Optimization, LLC, 2023) and MIS-specific solver KAMIS (Großmann et al., 2023) as the OR baselines, and the recent SA method iSCO (Sun et al., 2023) as a heuristic baseline. In the RL category, we include PPO (Ahn et al., 2020) and DIMES (Qiu et al., 2022). In the SL category, we have INTEL (Li et al., 2018b), DGL (Böther et al., 2022), and DIFUSCO (Sun & Yang, 2023). In the UL category, we use LTFT (Zhang et al., 2023) and DiffUCO (Sanokowski et al., 2024). For the non-MIS problems, the baselines include two OR methods, which are Gurobi and a semi-definite programming method (SDP); three heuristic methods, which are greedy, mean-filed annealing (MFA) (Bilbro et al., 1988) and iSCO (Sun et al., 2023); and three UL methods, which are ERDOES (Erdos & Rényi, 1984), LTFT (Zhang et al., 2023) and DiffUCO (Sanokowski et al., 2024), respectively. For most of those methods, we report their published results in Qiu et al. (2022); Zhang et al. (2023); Sun & Yang (2023); Sanokowski et al. (2024); Li et al. (2024). If a NN-based method has multiple variants, we only compare with the version with the longest running time (typically corresponding to the best result). For method iSCO, we run its code on our datasets as the time measurement in this work is inconsistent with others. For a fair

Table 1. Comparative results on the *Maximum Independent Set (MIS)* problem. On each dataset, we bold the best result and color the second-best one in green. By "best" or "second best", we exclude the OR solvers (Gurobi and KaMIS) as their running times are excessively large, preventing a fair comparison with the methods in other categories.

MIS		RB-[200–300]		RB-[800–1200]		ER-[700–800]		ER-[9000–11000]	
METHOD	TYPE	SIZE \uparrow	TIME \downarrow	SIZE \uparrow	TIME \downarrow	SIZE \uparrow	TIME \downarrow	SIZE \uparrow	TIME \downarrow
Gurobi	OR	19.98	47.57m	40.90	2.17h	41.38	50.00m	—	—
KaMIS	OR	20.10	1.40h	43.15	2.05h	44.87	52.13m	381.31	7.60h
PPO	RL	19.01	1.28m	32.32	7.55m	—	—	—	—
INTEL	SL	18.47	13.07m	34.47	20.28m	34.86	6.06m	284.63	5.02m
DGL	SL	17.36	12.78m	34.50	23.90m	37.26	22.71m	—	—
DIMES	RL	—	—	—	—	42.06	12.01m	332.80	12.72m
DIFUSCO	SL	18.52	16.05m	—	—	41.12	26.67m	—	—
LTFT	UL	19.18	32s	37.48	4.37m	—	—	—	—
DiffUCO	UL	19.24	54s	38.87	4.95m	—	—	—	—
iSCO	H	19.29	2.71m	36.96	11.26m	42.18	1.45m	365.37	1.10h
RLNN	RL	19.52	1.64m	38.46	6.24m	43.34	1.37m	363.34	11.76m
RLSA	H	19.97	35s	40.19	1.85m	44.10	20s	375.31	1.66m

Table 2. Comparative results on the *Max Clique (MCI)* and *Max Cut (MCut)* problems. On each dataset, we bold the best result and color the second-best one in green. By "best" or "second best", we exclude the OR solvers (Gurobi and KaMIS) as their running times are excessively large, preventing a fair comparison with the methods in other categories.

MCI		RB-[200–300]		RB-[800–1200]		MCut		BA-[200–300]		BA-[800–1200]	
METHOD	TYPE	SIZE \uparrow	TIME \downarrow	SIZE \uparrow	TIME \downarrow	METHOD	TYPE	SIZE \uparrow	TIME \downarrow	SIZE \uparrow	TIME \downarrow
Gurobi	OR	19.05	1m55s	33.89	19.67m	Gurobi	OR	730.87	8.50m	2944.38	1.28h
SDP	OR	—	—	—	—	SDP	OR	700.36	35.78m	2786.00	10.00h
Greedy	H	13.53	25s	26.71	25s	Greedy	H	688.31	13s	2786.00	3.12m
MFA	H	14.82	27s	27.94	2.32m	MFA	H	704.03	1.60m	2833.86	7.27m
ERDOES	UL	12.02	41s	25.43	2.27m	ERDOES	UL	693.45	46s	2870.34	2.82m
LTFT	UL	16.24	42s	31.42	4.83m	LTFT	UL	704.30	2.95m	2864.61	21.33m
DiffUCO	UL	16.22	1.00m	—	—	DiffUCO	UL	727.32	1.00m	2947.53	3.78m
iSCO	H	18.96	54s	40.35	11.37m	iSCO	H	728.24	1.67m	2919.97	4.18m
RLNN	RL	18.13	1.36m	35.23	7.83m	RLNN	RL	729.00	1.58m	2907.18	3.67m
RLSA	H	18.97	23s	40.53	1.27m	RLSA	H	733.54	27s	2955.81	1.45m

comparison, we run iSCO with the same number of steps and trials as we did for RLSA.

Implementation Details. We used two servers for the training of RLNN, one with 8 NVIDIA RTX A6000 GPUs, and the other one with 10 NVIDIA RTX 2080 Ti GPUs. All the time measurement is conducted on a single A6000 GPU. We find the efficiency of RLNN highly susceptible to the inductive bias of the NN architecture, e.g., a two-parameter linear model is enough to fit the gradient of MIS in Equation 15. Therefore, we mainly focus on verifying the effectiveness of RLNN algorithm, without optimizing the neural network architecture. In our experiment, we parameterized RLNN with a five-layer GCN (Kipf & Welling, 2017) with 128 hidden dimensions. Due to the increasing computational complexity at each step, we also accordingly reduce the number of sampling steps and trials of RLNN compared to RLSA, with other hyperparameters kept the

same. We include more details, such as the hyperparameters, in Appendix A

4.2. Main Results

In performance evaluation, we compare the mean value of the achieved problem-specific objective (larger is better) of each method on each problem, including the set size for MIS, clique size for MCI and cut size for MCut. In addition, we compare the *total running time* (lower is better) of each method on the entire test set by sequentially evaluating each instance. Since the OR solvers are guaranteed to find the optimal solution with enough running time, we do not include them for comparison.

Table 1 presents the results on the MIS problem. It can be seen that with a similar or even less running time, RLSA shows a significant improvement against the SOTA NN-based methods on RB and ER graphs. Besides, RLSA

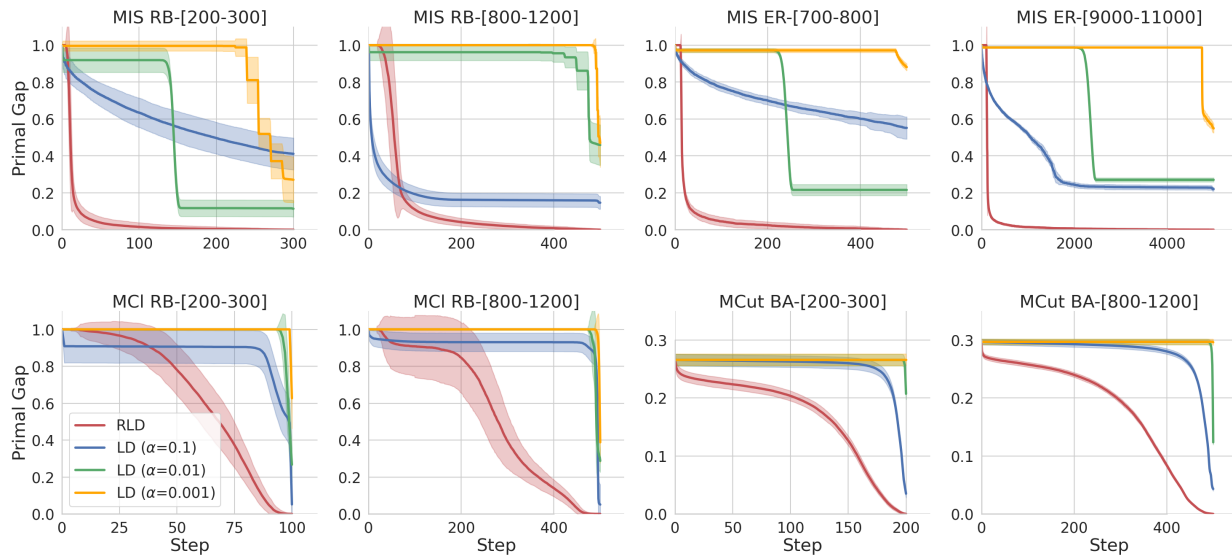


Figure 1. Comparison between RLD and standard discrete LD for SA. RLD/RLSA is in the red color. The mean value of the primal gap in the test set is plotted, while the shaded area indicates the standard deviation.

also consistently outperforms another gradient-guided SA method iSCO, with the same number of steps and trials. Due to the simplicity of RLSA, it only takes around 5-20% running time of iSCO, but with a better objective value. The performance of RLNN is also competitive, taking the second-best result on 2 out of 4 datasets. It also achieves the similar performance on ER-[900-11000] to iSCO, using less than 20% running time. Due to the significant increase in computational overhead at each step, RLNN only uses 10% number of trails and a shorter sampling chain compared to RLSA. We observe that RLNN could sometimes outperform RLSA with the same number of running steps and trials, which indicates the potential of NN in learning the problem distribution. But how to balance the computational resources between the per-step computation and searching efforts would be an interesting topic.

The comparative results on the MCI and MCut problems are summarized in Table 2. Generally, RLSA still maintains a clear efficiency advantage against iSCO. We observe that iSCO has a similar performance with RLSA on MCI at both scales, but RLSA and RLNN are still clearly better than other baselines. RLSA takes a consistent lead on MCut, while RLNN, DiffUCO and iSCO have a similar performance, with a significant improvement against other baselines.

Besides, we also include the comparative results between iSCO and RLSA with $10\times$ running steps in Appendix B, and the observation is consistent. In general, we find both RLSA and RLNN competitive on our evaluation benchmarks, and RLSA shows an impressive performance on all datasets with only a limited computational cost.

4.3. Ablation Study

To verify the effectiveness of regularization in RLD, we conduct the ablation study on RLSA and RLNN, respectively. We first compare RLD with the standard discrete LD (Zhang et al., 2022) for SA, searching the step size α over the set $\{0.1, 0.01, 0.001\}$. All other hyperparameters are kept the same as in RLSA. Figure 1 compares the dynamics of the primal gap (Berthold, 2014) across the sampling process. Here, the primal gap on each instance is defined as

$$\begin{cases} \frac{|H(\mathbf{x}) - H(\mathbf{x}^*)|}{\max\{|H(\mathbf{x})|, |H(\mathbf{x}^*)|\}}, & \text{if } H(\mathbf{x})H(\mathbf{x}^*) \geq 0; \\ 1, & \text{otherwise,} \end{cases} \quad (23)$$

where \mathbf{x} corresponds to the best solution found so far and \mathbf{x}^* is a pre-computed optimal (or best known) solution.

It can be seen that the standard discrete LD always ends up at a sub-optimal solution except on MCI. The searching could easily get stuck in a local optima, indicated by the flat stage. In contrast, RLSA usually converges in just a few steps (less than 100) without getting stuck in any local optima. Note that our searching set has already covered the most common choices of the gradient descent step size for continuous data, and a smaller step size, e.g., 0.001, shows an even worse performance. Contrast to the optimization in the continuous domain, CO clearly presents a different challenge and we address it by RLD.

We then examine the regularization term in Equation 20 for training RLNN. We perform the ablation study on small-scale graphs by training RLNN without regularization, and present the comparative results in Table 3. The regularization brings a significant improvement on RLNN in most

Table 3. Ablation Study on regularization in RLNN. The numbers correspond to the set size (larger is better).

METHOD	MIS		MCI	MCut
	RB-[200-300]	ER-[700-800]	RB-[200-300]	BA-[200-300]
RLNN w/o regularization	18.64	37.73	16.62	730.20
RLNN w/ regularization	19.52	43.34	18.13	729.00

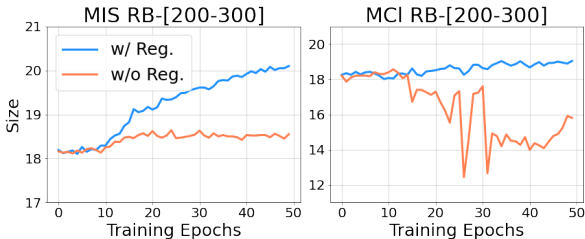


Figure 2. Training curves of RLNN with or without regularization. Validation performance (set/cliue size) is shown.

cases, except on MCut. We hypothesize this is because MCut has no constraint and suffers less from the local optima. But on other benchmarks, we find it almost impossible to effectively train RLNN without regularization. Here we visualize training dynamics on MIS and MCI by plotting the set/cliue size on the validation set (larger is better) in Figure 2. It can be seen that the performance of the orange curve (no regularization) remains unchanged (on MIS) or even drops after more training epochs (on MCI). The usage of a local optimization loss function makes the diversity of training samples a huge concern. While the regularization would enforce RLNN to collect different training samples and encourage the search during inference time. The similar spirit is also used in some well-known reinforcement learning algorithms to encourage the exploration, such as the curiosity (Pathak et al., 2017) and soft policies (Haarnoja et al., 2017; 2018).

5. Related Work

5.1. Neural Solvers for Combinatorial Optimization

The neural network (NN) models have recently garnered vast attention in solving CO problem (Bengio et al., 2020). The NN-based solvers could be roughly categorized into three classes according to the training methods, including the supervised learning-based (Li et al., 2018a; Gasse et al., 2019; Sun & Yang, 2023; Li et al., 2023; 2024), unsupervised learning-based (Karalias & Loukas, 2020a; Wang et al., 2022; Wang & Li, 2023; Zhang et al., 2023; Sanokowski et al., 2024), and reinforcement learning-based (Khalil et al., 2017; Qiu et al., 2022) methods. Our proposed RLNN method is partially based on reinforcement learning, but could be efficiently trained with a local objective. Such a feature has greatly improved its training efficiency by

eliminating the need to estimate the future return.

5.2. Sampling for Combinatorial Optimization

Sampling-based methods (Metropolis et al., 1953; Hastings, 1970; Neal, 1996; IBA, 2001) have been commonly applied in CO problems (WANG et al., 2009; Bhattacharya et al., 2014; Tavakkoli-Moghaddam et al., 2007; Seçkiner & Kurt, 2007; Chen & Ke, 2004). However, earlier methods often encountered slow convergence compared to learning-based approaches due to an inefficient proposal. Recent advancements in discrete Monte Carlo Markov Chain (Grathwohl et al., 2021; Zhang et al., 2022; Sun et al., 2022) have revitalized sampling-based methods and Sun et al. (2023) demonstrated that simulated annealing (SA) can surpass neural CO solvers. In this work, we have advanced the current study on discrete Langevin dynamics, and proposed a novel SA algorithm. Our conclusion supports the previous study the further advances the development of the field.

6. Conclusion & Limitation

In this work, we point out the difference in local optimal between continuous optimization and continuous optimization (CO), and propose a novel sampling framework called Regularized Langevin Dynamics (RLD) to tackle the issue in CO. On top of that, we develop two CO solvers, one based on simulated annealing (SA), and the other one based on neural networks. Our empirical evaluation on three classical CO problems demonstrate that our proposed methods can achieve the state-of-the-art (SOTA) or near-SOTA performance with high efficiency. Especially, our proposed SA method consistently outperforms the previous SA baseline using only 20% running time. In summary, RLD is a simple yet effective framework, showing a strong potential in addressing CO problems.

In this work, we only consider binary data for ease of analysis. Although the whole framework could be generalized, its effectiveness remains unclear on other CO problems with integer or mixed integer variables. Future work may extend it to more real-world CO problems by taking other conditions into consideration. Besides, we have given an intuitive explanation of RLD in this work, but the theoretical understanding of RLD is generally missing. We also expect to address this part in our future work.

Impact Statement

This paper presents work whose goal is to advance the field of Machine Learning. There are many potential societal consequences of our work, none which we feel must be specifically highlighted here.

References

- Ahn, S., Seo, Y., and Shin, J. Learning what to defer for maximum independent sets. In *Proceedings of the 37th International Conference on Machine Learning, ICML'20*. JMLR.org, 2020.
- Austin, J., Johnson, D. D., Ho, J., Tarlow, D., and van den Berg, R. Structured denoising diffusion models in discrete state-spaces. In Beygelzimer, A., Dauphin, Y., Liang, P., and Vaughan, J. W. (eds.), *Advances in Neural Information Processing Systems*, 2021. URL <https://openreview.net/forum?id=h7-XixPCAL>.
- Barabási, A.-L. and Albert, R. Emergence of scaling in random networks. *Science*, 286(5439): 509–512, 1999. doi: 10.1126/science.286.5439.509. URL <https://www.science.org/doi/abs/10.1126/science.286.5439.509>.
- Bengio, Y., Lodi, A., and Prouvost, A. Machine learning for combinatorial optimization: a methodological tour d’horizon, 2020.
- Berthold, T. Heuristic algorithms in global minlp solvers. 2014. URL <https://api.semanticscholar.org/CorpusID:124820186>.
- Bhattacharya, A., Ghatak, S., Ghosh, S., Das, R. K., and Bengal, W. Simulated annealing approach onto vlsi circuit partitioning. 2014. URL <https://api.semanticscholar.org/CorpusID:33197762>.
- Bilbro, G., Mann, R., Miller, T., Snyder, W., van den Bout, D., and White, M. Optimization by mean field annealing. In Touretzky, D. (ed.), *Advances in Neural Information Processing Systems*, volume 1. Morgan-Kaufmann, 1988. URL https://proceedings.neurips.cc/paper_files/paper/1988/file/ec5decca5ed3d6b8079e2e7e7bacc9f2-Paper.pdf.
- Böther, M., Kißig, O., Taraz, M., Cohen, S., Seidel, K., and Friedrich, T. What’s wrong with deep learning in tree search for combinatorial optimization. In *International Conference on Learning Representations*, 2022. URL <https://openreview.net/forum?id=mk0HzdqY7il>.
- Bradbury, J., Frostig, R., Hawkins, P., Johnson, M. J., Leary, C., Maclaurin, D., Necula, G., Paszke, A., VanderPlas, J., Wanderman-Milne, S., and Zhang, Q. JAX: composable transformations of Python+NumPy programs, 2018. URL <http://github.com/google/jax>.
- Chen, T., ZHANG, R., and Hinton, G. Analog bits: Generating discrete data using diffusion models with self-conditioning. In *The Eleventh International Conference on Learning Representations*, 2023. URL <https://openreview.net/forum?id=3itjR9QxFw>.
- Chen, Y. L. and Ke, Y.-L. Multi-objective var planning for large-scale power systems using projection-based two-layer simulated annealing algorithms. 2004. URL <https://api.semanticscholar.org/CorpusID:119669727>.
- Chopra, S. and Meindl, P. Strategy, planning, and operation. *Supply Chain Management*, 15(5):71–85, 2001.
- Cortés, J. Finite-time convergent gradient flows with applications to network consensus. *Automatica*, 42:1993–2000, 11 2006. doi: 10.1016/j.automatica.2006.06.015.
- Erdos, P. L. and Rényi, A. On the evolution of random graphs. *Transactions of the American Mathematical Society*, 286:257–257, 1984. URL <https://api.semanticscholar.org/CorpusID:6829589>.
- Ernst, A. T., Jiang, H., Krishnamoorthy, M., and Sier, D. Staff scheduling and rostering: A review of applications, methods and models. *European journal of operational research*, 153(1):3–27, 2004.
- Fey, M. and Lenssen, J. E. Fast graph representation learning with PyTorch Geometric. In *ICLR Workshop on Representation Learning on Graphs and Manifolds*, 2019.
- Gasse, M., Chételat, D., Ferroni, N., Charlin, L., and Lodi, A. Exact combinatorial optimization with graph convolutional neural networks. In *Advances in Neural Information Processing Systems 32*, 2019.
- Grathwohl, W., Swersky, K., Hashemi, M., Duvenaud, D. K., and Maddison, C. J. Oops i took a gradient: Scalable sampling for discrete distributions. *ArXiv*, abs/2102.04509, 2021. URL <https://api.semanticscholar.org/CorpusID:231855281>.
- Großmann, E., Lamm, S., Schulz, C., and Strash, D. Finding near-optimal weight independent sets at scale. In *Proceedings of the Genetic and Evolutionary Computation Conference, GECCO '23*, pp. 293–302, New York, NY, USA, 2023. Association for Computing Machinery. ISBN 9798400701191. doi: 10.1145/3583131.3590353. URL <https://doi.org/10.1145/3583131.3590353>.

- Gugger, S., Debut, L., Wolf, T., Schmid, P., Mueller, Z., Mangrulkar, S., Sun, M., and Bossan, B. Accelerate: Training and inference at scale made simple, efficient and adaptable. <https://github.com/huggingface/accelerate>, 2022.
- Gurobi Optimization, LLC. Gurobi Optimizer Reference Manual, 2023. URL <https://www.gurobi.com>.
- Gusfield, D. Algorithms on stings, trees, and sequences: Computer science and computational biology. *Acm Sigact News*, 28(4):41–60, 1997.
- Haarnoja, T., Tang, H., Abbeel, P., and Levine, S. Reinforcement learning with deep energy-based policies. 2017.
- Haarnoja, T., Zhou, A., Abbeel, P., and Levine, S. Soft actor-critic: Off-policy maximum entropy deep reinforcement learning with a stochastic actor. In Dy, J. and Krause, A. (eds.), *Proceedings of the 35th International Conference on Machine Learning*, volume 80 of *Proceedings of Machine Learning Research*, pp. 1861–1870. PMLR, 10–15 Jul 2018. URL <https://proceedings.mlr.press/v80/haarnoja18b.html>.
- Hastings, W. K. Monte carlo sampling methods using markov chains and their applications. *Biometrika*, 57:97–109, 1970. URL <https://api.semanticscholar.org/CorpusID:21204149>.
- Ho, J., Jain, A., and Abbeel, P. Denoising diffusion probabilistic models. In Larochelle, H., Ranzato, M., Hadsell, R., Balcan, M., and Lin, H. (eds.), *Advances in Neural Information Processing Systems*, volume 33, pp. 6840–6851. Curran Associates, Inc., 2020. URL https://proceedings.neurips.cc/paper_files/paper/2020/file/4c5bcfec8584af0d967f1ab10179ca4b-Paper.pdf.
- IBA, Y. Extended ensemble monte carlo. *International Journal of Modern Physics C*, 12(05):623–656, June 2001. ISSN 1793-6586. doi: 10.1142/S0129183101001912. URL <http://dx.doi.org/10.1142/S0129183101001912>.
- Johnson, D. S., Aragon, C. R., McGeoch, L. A., and Schevon, C. Optimization by simulated annealing: An experimental evaluation; part ii, graph coloring and number partitioning. *Operations Research*, 39(3):378–406, 1991. ISSN 0030364X, 15265463. URL <http://www.jstor.org/stable/171393>.
- Karalias, N. and Loukas, A. Erdos goes neural: an unsupervised learning framework for combinatorial optimization on graphs. *ArXiv*, abs/2006.10643, 2020a. URL <https://api.semanticscholar.org/CorpusID:219792252>.
- Karalias, N. and Loukas, A. Erdos goes neural: an unsupervised learning framework for combinatorial optimization on graphs. In Larochelle, H., Ranzato, M., Hadsell, R., Balcan, M., and Lin, H. (eds.), *Advances in Neural Information Processing Systems*, volume 33, pp. 6659–6672. Curran Associates, Inc., 2020b. URL https://proceedings.neurips.cc/paper_files/paper/2020/file/49f85a9ed090b20c8bed85a5923c669f-Paper.pdf.
- Khalil, E., Dai, H., Zhang, Y., Dilkina, B., and Song, L. Learning combinatorial optimization algorithms over graphs. In Guyon, I., Luxburg, U. V., Bengio, S., Wallach, H., Fergus, R., Vishwanathan, S., and Garnett, R. (eds.), *Advances in Neural Information Processing Systems*, volume 30. Curran Associates, Inc., 2017. URL https://proceedings.neurips.cc/paper_files/paper/2017/file/d9896106ca98d3d05b8cbdf4fd8b13a1-Paper.pdf.
- Kipf, T. N. and Welling, M. Semi-supervised classification with graph convolutional networks. In *International Conference on Learning Representations*, 2017. URL <https://openreview.net/forum?id=SJU4ayYgl>.
- Kirkpatrick, S., Gelatt, C. D., and Vecchi, M. P. Optimization by simulated annealing. *Science*, 220(4598):671–680, 1983. doi: 10.1126/science.220.4598.671. URL <https://www.science.org/doi/abs/10.1126/science.220.4598.671>.
- Kool, W., van Hoof, H., and Welling, M. Attention, learn to solve routing problems! In *International Conference on Learning Representations*, 2019. URL <https://openreview.net/forum?id=ByxBFsRqYm>.
- Lecun, Y., Chopra, S., and Hadsell, R. *A tutorial on energy-based learning*. 01 2006.
- Li, Y., Guo, J., Wang, R., and Yan, J. From distribution learning in training to gradient search in testing for combinatorial optimization. In *Thirty-seventh Conference on Neural Information Processing Systems*, 2023. URL <https://openreview.net/forum?id=JtF0ugNMv2>.
- Li, Y., Guo, J., Wang, R., Zha, H., and Yan, J. Fast t2t: Optimization consistency speeds up diffusion-based training-to-testing solving for combinatorial optimization. In *The Thirty-eighth Annual Conference on Neural Information Processing Systems*, 2024. URL <https://openreview.net/forum?id=xDrKZOZEoc>.
- Li, Z., Chen, Q., and Koltun, V. Combinatorial optimization with graph convolutional networks and guided

- tree search. In *Neural Information Processing Systems*, 2018a. URL <https://api.semanticscholar.org/CorpusID:53027872>.
- Li, Z., Chen, Q., and Koltun, V. Combinatorial optimization with graph convolutional networks and guided tree search. In Bengio, S., Wallach, H., Larochelle, H., Grauman, K., Cesa-Bianchi, N., and Garnett, R. (eds.), *Advances in Neural Information Processing Systems*, volume 31. Curran Associates, Inc., 2018b. URL https://proceedings.neurips.cc/paper_files/paper/2018/file/8d3bba7425e7c98c50f52calb52d3735-Paper.pdf.
- Lobo, M. S., Fazel, M., and Boyd, S. Portfolio optimization with linear and fixed transaction costs. *Annals of Operations Research*, 152:341–365, 2007.
- Lucas, A. Ising formulations of many np problems. *Frontiers in Physics*, 2, 2014. ISSN 2296-424X. doi: 10.3389/fphy.2014.00005. URL <https://www.frontiersin.org/journals/physics/articles/10.3389/fphy.2014.00005>.
- Metropolis, N. C., Rosenbluth, A. W., Rosenbluth, M. N., and Teller, A. H. Equation of state calculations by fast computing machines. *Journal of Chemical Physics*, 21:1087–1092, 1953. URL <https://api.semanticscholar.org/CorpusID:1046577>.
- Neal, R. M. Sampling from multimodal distributions using tempered transitions. *Statistics and Computing*, 6:353–366, 1996. URL <https://api.semanticscholar.org/CorpusID:11106113>.
- Papadimitriou, C. and Steiglitz, K. *Combinatorial Optimization: Algorithms and Complexity*, volume 32. 01 1982. ISBN 0-13-152462-3. doi: 10.1109/TASSP.1984.1164450.
- Papadimitriou, C. H. and Steiglitz, K. *Combinatorial optimization: algorithms and complexity*. Courier Corporation, 1998.
- Paszke, A., Gross, S., Chintala, S., Chanan, G., Yang, E., DeVito, Z., Lin, Z., Desmaison, A., Antiga, L., and Lerer, A. Automatic differentiation in pytorch. 2017.
- Pathak, D., Agrawal, P., Efros, A. A., and Darrell, T. Curiosity-driven exploration by self-supervised prediction. In *International Conference on Machine Learning (ICML)*, 2017.
- Qiu, R., Sun, Z., and Yang, Y. DIMES: A differentiable meta solver for combinatorial optimization problems. In Oh, A. H., Agarwal, A., Belgrave, D., and Cho, K. (eds.), *Advances in Neural Information Processing Systems*, 2022. URL <https://openreview.net/forum?id=9u05zr0nhx>.
- Rubinstein, M. Markowitz’s” portfolio selection”: A fifty-year retrospective. *The Journal of finance*, 57(3):1041–1045, 2002.
- Sanokowski, S., Hochreiter, S., and Lehner, S. A diffusion model framework for unsupervised neural combinatorial optimization. In *ICML*, 2024. URL <https://openreview.net/forum?id=AFfXlKFHXJ>.
- Seçkiner, S. U. and Kurt, M. A simulated annealing approach to the solution of job rotation scheduling problems. *Applied Mathematics and Computation*, 188(1):31–45, 2007. ISSN 0096-3003. doi: <https://doi.org/10.1016/j.amc.2006.09.082>. URL <https://www.sciencedirect.com/science/article/pii/S0096300306013166>.
- Sohl-Dickstein, J., Weiss, E., Maheswaranathan, N., and Ganguli, S. Deep unsupervised learning using nonequilibrium thermodynamics. In Bach, F. and Blei, D. (eds.), *Proceedings of the 32nd International Conference on Machine Learning Research*, volume 37 of *Proceedings of Machine Learning Research*, pp. 2256–2265, Lille, France, 07–09 Jul 2015. PMLR. URL <https://proceedings.mlr.press/v37/sohl-dickstein15.html>.
- Song, Y. and Ermon, S. Generative modeling by estimating gradients of the data distribution. In *Advances in Neural Information Processing Systems*, pp. 11895–11907, 2019.
- Song, Y. and Ermon, S. Improved techniques for training score-based generative models. *Advances in neural information processing systems*, 33:12438–12448, 2020.
- Sun, H., Dai, H., Xia, W., and Ramamurthy, A. Path auxiliary proposal for MCMC in discrete space. In *International Conference on Learning Representations*, 2022. URL <https://openreview.net/forum?id=JSR-YDImK95>.
- Sun, H., Goshvadi, K., Nova, A., Schuurmans, D., and Dai, H. Revisiting sampling for combinatorial optimization. In Krause, A., Brunskill, E., Cho, K., Engelhardt, B., Sabato, S., and Scarlett, J. (eds.), *Proceedings of the 40th International Conference on Machine Learning Research*, volume 202 of *Proceedings of Machine Learning Research*, pp. 32859–32874. PMLR, 23–29 Jul 2023. URL <https://proceedings.mlr.press/v202/sun23c.html>.
- Sun, Z. and Yang, Y. DIFUSCO: Graph-based diffusion solvers for combinatorial optimization. In *Thirty-seventh Conference on Neural Information Processing Systems*, 2023. URL <https://openreview.net/forum?id=JV8Ff0lgVV>.

- Tavakkoli-Moghaddam, R., Safaei, N., Kah, M., and Rabbani, M. A new capacitated vehicle routing problem with split service for minimizing fleet cost by simulated annealing. *Journal of the Franklin Institute*, 344(5):406–425, 2007. ISSN 0016-0032. doi: <https://doi.org/10.1016/j.jfranklin.2005.12.002>. URL <https://www.sciencedirect.com/science/article/pii/S0016003205001171>. Modeling, Simulation and Applied Optimization Part II.
- Trofin, M., Qian, Y., Brevdo, E., Lin, Z., Choromanski, K., and Li, D. Mlgo: a machine learning guided compiler optimizations framework. *arXiv preprint arXiv:2101.04808*, 2021.
- WANG, C., HYMAN, J. D., PERCUS, A., and CAFLISCH, R. Parallel tempering for the traveling salesman problem. *International Journal of Modern Physics C*, 20(04):539–556, 2009. doi: 10.1142/S0129183109013893. URL <https://doi.org/10.1142/S0129183109013893>.
- Wang, H. P. and Li, P. Unsupervised learning for combinatorial optimization needs meta learning. In *The Eleventh International Conference on Learning Representations*, 2023. URL <https://openreview.net/forum?id=-ENYHCE8zBp>.
- Wang, H. P., Wu, N., Yang, H., Hao, C., and Li, P. Unsupervised learning for combinatorial optimization with principled objective relaxation. In Oh, A. H., Agarwal, A., Belgrave, D., and Cho, K. (eds.), *Advances in Neural Information Processing Systems*, 2022. URL https://openreview.net/forum?id=HjNn9oD_v47.
- Welling, M. and Teh, Y. W. Bayesian learning via stochastic gradient langevin dynamics. In *Proceedings of the 28th International Conference on International Conference on Machine Learning, ICML'11*, pp. 681–688, Madison, WI, USA, 2011. Omnipress. ISBN 9781450306195.
- Xu, K. and Li, W. Exact phase transitions in random constraint satisfaction problems. *ArXiv*, cs.AI/0004005, 2000. URL <https://api.semanticscholar.org/CorpusID:2407346>.
- Zanella, G. Informed proposals for local mcmc in discrete spaces. *Journal of the American Statistical Association*, 115:852 – 865, 2017. URL <https://api.semanticscholar.org/CorpusID:88514775>.
- Zhang, D., Dai, H., Malkin, N., Courville, A., Bengio, Y., and Pan, L. Let the flows tell: Solving graph combinatorial problems with GFlownets. In *Thirty-seventh Conference on Neural Information Processing Systems*, 2023. URL <https://openreview.net/forum?id=sTjw3JHs2V>.
- Zhang, R., Liu, X., and Liu, Q. A langevin-like sampler for discrete distributions. *International Conference on Machine Learning*, 2022.
- Zheng, L., Li, Z., Zhang, H., Zhuang, Y., Chen, Z., Huang, Y., Wang, Y., Xu, Y., Zhuo, D., Xing, E. P., et al. Alpa: Automating inter-and {Intra-Operator} parallelism for distributed deep learning. In *16th USENIX Symposium on Operating Systems Design and Implementation (OSDI 22)*, pp. 559–578, 2022.

A. Additional Experiment Details

A.1. Hyperparameters

We include the hyperparameters of RLSA and RLNN in Table 4 and 5, respectively. The initial temperature τ_0 is randomly searched in the range of 0.001 to 10, and the step size is randomly searched in the range of 2 to 100. In general, larger K and T always lead to a better performance, so we simply control them such that the running time of RLSA is similar to the fastest baseline. For RLNN, we allow for more time budget, just controlling its K and T such that its running time is comparable to most baselines.

Table 4. Hyperparameters used by RLSA on all datasets.

Problem	Dataset	τ_0	d	K	T	β
MIS	RB-[200-300]	0.01	5	200	300	1.02
	RB-[800-1200]	0.01	5	200	500	1.02
	ER-[700-800]	0.01	20	200	500	1.001
	ER-[9000-1100]	0.01	20	200	5000	1.001
MCI	RB-[200-300]	4	2	200	100	1.02
	RB-[800-1200]	4	2	200	500	1.02
MCut	BA-[200-300]	5	20	200	200	1.02
	BA-[800-1200]	5	20	200	500	1.02

Table 5. Hyperparameters used by RLNN on all datasets.

Problem	Dataset	τ_0	d	K	T	β	K'	T'	λ
MIS	RB-[200-300]	1	5	20	100	1.02	10	50	0.5
	RB-[800-1200]	1	5	20	200	1.02	10	300	0.5
	ER-[700-800]	1	20	20	200	1.001	10	500	0.5
	ER-[9000-1100]	1	20	20	800	1.001	—	—	—
MCI	RB-[200-300]	1	2	20	100	1.02	10	100	0.5
	RB-[800-1200]	1	2	20	200	1.02	10	300	0.5
MCut	BA-[200-300]	1	20	20	100	1.02	10	50	0.5
	BA-[800-1200]	1	20	20	200	1.02	10	300	0.5

A.2. Training

RLNN is parameterized by a five-layer GCN (Welling & Teh, 2011) with 128 hidden dimensions. A linear layer is first used to project the input solution \mathbf{x} into a 128-dim embedding \mathbf{H}^0 . Each layer of GCN performs the following update:

$$\mathbf{H}^{l+1} = \sigma(\mathbf{U}^l \mathbf{H}^l + \mathbf{V}^l \mathbf{D}^{-1/2} \hat{\mathbf{A}} \mathbf{D}^{-1/2} \mathbf{H}^l) + \mathbf{H}^l, \quad (24)$$

where \mathbf{U}^l and \mathbf{V}^l are model parameters, $\hat{\mathbf{A}} = \mathbf{A} + \mathbf{I}_{N \times N}$ is the adjacency matrix with the self loop, \mathbf{D} is a diagonal degree matrix with $\mathbf{D}_{ii} = \sum_j 1^N \hat{\mathbf{A}}_{ij}$, and σ is the activation function. We use ReLU as the activation function for all layers. The output hidden vector is projected by a final linear layer into the single dimension. A sigmoid function is then applied to generate the flipping probability $q_\theta(\mathbf{x}'_i = 1 - \mathbf{x}_i | \mathbf{x})$.

We train RLNN with 50 epochs in all data sets except RB- [700–800] for MCI, where we use 80 epochs since we notice that the training does not converge at 50 epochs. On each graph, we sample K' trajectories with T' lengths, which amounts to $K'T'$ samples to train on. The batch size is set as 32 per GPU, and an Adam optimizer is used for optimization, with a learning rate of 0.0001.

In terms of the training time, all experiments can finish under 1 hour on our server with 8 RTX A6000 GPUs. The large-scale graphs and ER-[700-800] graphs may need 3 hours to finish on our server with 10 RTX 2080 Ti GPUs. Our implementation is based on PyTorch Geometric (Fey & Lenssen, 2019) and accelerate (Gugger et al., 2022).

During our inference time, we use the float16 data type to store the tensor, which accelerates the tensor product. But in general, we find our method way more efficient than our baselines even without this technique.

A.3. Postprocessing

We postprocess the best solutions (with the lowest energy) on MIS and MCI problems to satisfy the constraint. We find our method almost surely yields a valid solution, so we just adopt the simplest way to greedily decode it. On MIS, we sort all nodes according to its value (0 or 1) and initialize the candidate set with all nodes. Each time we select a node, we remove itself and all its neighbors from the candidate set and repeat the process until no candidates are available. On MCI, we perform a similar process by selecting a node and removing itself and all the nodes not in its neighborhood set. on MCut, we simply return the best solution since the problem is not constrained.

B. Comparison under More Running Steps

Here we compare iSCO (Sun et al., 2023) and RLSA by running both methods with 10× more steps in Table 6 and 7. Although iSCO has achieved a very close performance to RLSA in some small-scale datasets, RLSA still maintains a clear advantage on large-scale datasets, with significantly less running time.

In particular, we note that RLSA has already achieved comparable performance to the exact solvers over multiple benchmarks in Table 1 and 2, especially on the large-scale problems. This has demonstrated the strong power of RLSA in CO.

Table 6. Comparative results between iSCO and RLSA with 10 times more steps on MIS. The best one is bolded.

MIS		RB-[200–300]		RB-[800–1200]		ER-[700–800]		ER-[9000–11000]	
METHOD	TYPE	SIZE ↑	TIME ↓	SIZE ↑	TIME ↓	SIZE ↑	TIME ↓	SIZE ↑	TIME ↓
iSCO (10×)	H	20.01	26.25m	40.47	1.87h	44.41	7.21m	378.56	11.03h
RLSA (10×)	H	20.10	6.98m	41.83	10.65m	45.05	2.92m	379.19	17.63m

Table 7. Comparative results between iSCO and RLSA with 10 times more steps on MCI and MCut. The best one is bolded.

MCI		RB-[200–300]		RB-[800–1200]		MCut		BA-[200–300]		BA-[800–1200]	
METHOD	TYPE	SIZE ↑	TIME ↓	SIZE ↑	TIME ↓	METHOD	TYPE	SIZE ↑	TIME ↓	SIZE ↑	TIME ↓
iSCO (10×)	H	18.97	8.81m	40.41	1.83h	iSCO (10×)	H	734.62	1.20h	2960.23	43.98m
RLSA (10×)	H	18.97	3.14m	40.63	8.67m	RLSA (10×)	H	734.62	4.07m	2968.59	10.25m

C. Example Code for RLSA

The following Python code outlines our implementation of RLSA. The energy function corresponds to the formulas in Section 3.2 and the input parameters are in summarized in Section A. In our experiments, the time measurement corresponds to the running time of the entire RLSA function below.

```

1 def energy_func(A, b, x, penalty_coeff=1.02):
2     """
3     The energy function is:  $b^T x + \text{penalty\_coeff} * x^T A x$ 
4     Return the energy and the gradient
5     """
6
7     L = A @ x
8     energy = torch.sum(x * (penalty_coeff * L + b), dim=0)
9     grad = 2 * penalty_coeff * L + b
10
11     return energy, grad
12
13 def RLSA(graph, tau0, step_size, num_runs, num_steps, penalty_coeff):
14     """
15     graph: the graph object in torch_geometric
16     num_runs: the number of parallel SA processes

```

```

17 num_steps: the number of SA steps
18 tau0: the initial temperature
19 """
20
21 # initialization
22 num_nodes = graph.num_nodes
23
24 A = torch.sparse_coo_tensor(
25     graph.edge_index,
26     graph.edge_weight,
27     torch.Size((num_nodes, num_nodes))
28 )
29 x = torch.randint(0,2, (num_nodes, num_runs))
30
31 energy, grad = energy_func(A, graph.b, x, penalty_coeff)
32 best_energy = energy
33 best_sol = x.clone()
34
35 # SA
36 for epoch in range(num_steps):
37     # annealing
38     tau = tau0*(1-epoch/num_steps)
39
40     # sampling
41     delta = grad*(2*x-1)/2
42     term2 = -torch.kthvalue(
43         -delta,
44         step_size,
45         dim=0,
46         keepdim=True
47     ).values
48
49     flip_prob = torch.sigmoid((delta-term2)/tau)
50     rr = torch.rand_like(x.data)
51     x = torch.where(rr<flip_prob, 1-x, x)
52
53     # update loss
54     energy, grad = energy_func(A, graph.b, x, penalty_coeff)
55     to_update = energy<best_energy
56     best_sol[:,to_update] = x[:,to_update]
57     best_energy[to_update] = energy[to_update]
58
59 return best_energy, best_sol

```